Error

An error occurred while processing this page. See the system log for more details.

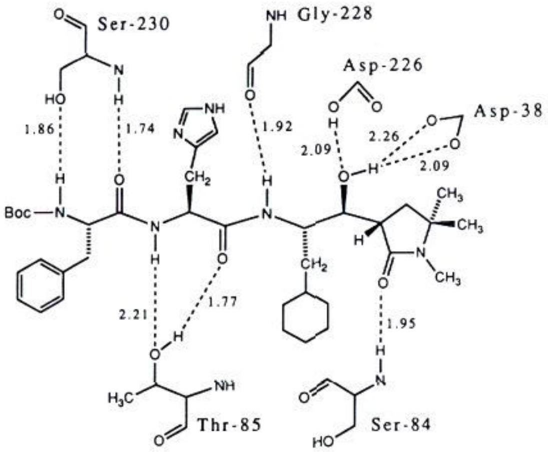

Figure 8. Schematic representation of the hydrogen-bond network of **34** in the human renin model. Distances are in angstroms.

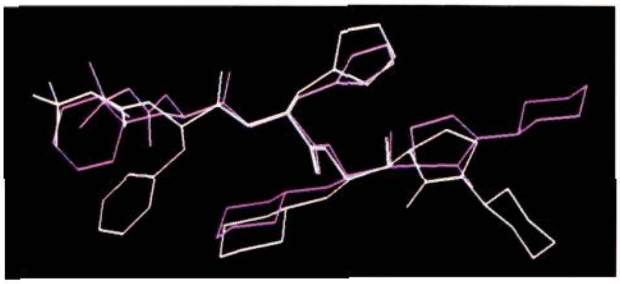

Figure 9. Superposition of the solid-state conformation of **36** (purple) and the modeled enzyme-bound conformation (yellow).

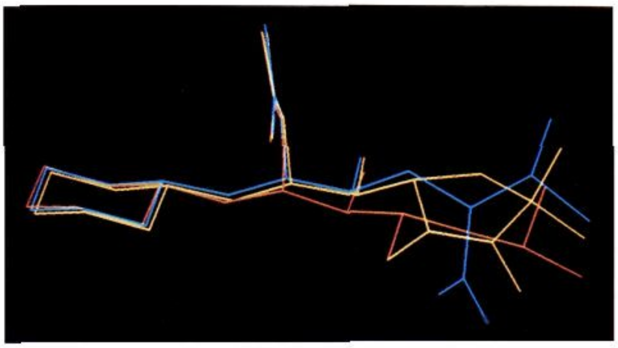

Figure 10. Superposition of the modeled enzyme bound conformations of **34** (yellow), alkyl diol **43** (red), and hydroxyethylene isostere **42** (blue) C-termini. The 2-methylbutyl side chain of **42** has been omitted for clarity.

with the sequences of the fungal proteases. The aligned human sequence was then mapped onto the superimposed X-ray structures of the fungal aspartyl proteases. The structurally conserved regions were taken from the rhizopuspepsin X-ray structure while the variable regions were taken from protease structure whose sequence best aligned with the human sequence in that region. Coordinates for the renin model are available in Protein Data Bank format as supplementary material. X-ray structures for several fungal enzyme–inhibitor complexes[25] provided a starting conformation for docking the ACHPA–lactam inhibitors in the human renin model. Molecular geometries for the docked inhibitors were created with the Merck molecular modeling system MOLEDIT[26] and were energy minimized in the static active site by using OPTIMOL, a modified MM2 force field program.[27]

Comparison of the docked conformations of **34** and residues 7–13 of angiotensinogen in which the Leu^{10} amide carbonyl is hydrated produced a good overlap of the *gem*-dimethyl group in **34** with the Val^{11} side chain, suggesting that the increased potency of **34** compared to that of **8c** is the result of incorporating a P$_1$′ side chain mimic. Additionally, the lactam carbonyl oxygen in the docked conformation of **34** is within hydrogen bonding distance to the backbone N–H of Ser^{84} in the "flap" region of the enzyme. Graphic and schematic representations of the enzyme-bound form of **34** are given in Figures 7 and 8, respectively. This model of the enzyme–inhibitor complex is consistent with the experimental data obtained for the epimerically related inhibitors **8a** and **8c** in that the poorly binding epimer **8a** which has the "wrong" chirality at C2 (IC$_{50}$ > 20 000 nM) cannot form the aforementioned hydrogen bond to the flap without the rest of the lactam ring encountering unfavorable van der Waals contacts with the enzyme. The substituent on the lactam nitrogen of **34** can be oriented in a direction away from the binding cleft, an arrangement which is consistent with the experimental results for inhibitors **35–40** that indicate a tolerance for a wide variety of substituents at this position. The binding model, however, does not adequately account for the trend in potency observed for inhibitors **30–33** in that the enzyme model provides a steric environment around the face of the lactam bearing the 5-position substituent that should accommodate groups larger than ethyl. This area in the human enzyme model contains a polyproline sequence (residues 306–311) that is not found in the fungal enzymes, and the results for inhibitors **30–33** suggest that this region of the model may need modification.

The solid-state conformation of inhibitor **36** obtained by single-crystal X-ray diffraction analysis shows a remarkable similarity to the enzyme-bound conformation obtained by using our renin model (Figure 9). Rotations of 60° and 95° about the Phe ψ and ACHPA–lactam C2–C3 bonds, respectively, in the solid-state conformer produces a backbone conformation which closely resembles that of the modeled bound conformer. To the extent that the observed solid-state conformation of **36** might resemble its solution conformation, our model of the enzyme–inhibitor complex suggests that only a minimal amount of torsional reorganization would be required to adopt a good conformation for binding to the enzyme.

The in vitro potency of the optimized ACHPA–lactam inhibitor **34** is very similar to inhibitors that contain hydroxyethylene isostere and alkyl diol[28j] non-peptide C-

---

[25] (a) Foundling, S. I.; Cooper, J.; Watson, F. E.; Cleasby, A.; Pearl, L. H.; Sibanda, B. L.; Hemmings, A.; Wood, S. P.; Blundell, T. L.; Valler, M. J.; Norey, C. G.; Kay, J.; Boger, J.; Dunn, B. M.; Leckie, B. J.; Jones, D. M.; Atrash, B.; Hallet, A.; Szelke, M. *Nature* **1987**, *327*, 349. (b) Davies, D.; Suguna, K. Preliminary coordinate sets for enzyme-inhibitor complexes of rhizopuspepsin were graciously provided.

[26] Gund, P.; Andose, J. D.; Rhodes, J. B.; Smith, G. M. *Science* **1980**, *208*, 1425. (b) Smith, G. M.; Hangauer, D. G.; Andose, J. D.; Bush, B. L.; Fluder, E. M.; Gund, P.; McIntyre, E. F. *Drug. Inf. J.* **1984**, *18*, 167.

[27] Halgren, T. A.; Merck, Sharpe and Dohme Research Laboratories, Rahway, NJ; unpublished work on the development of the force field program OPTIMOL. OPTIMOL differs from MM2 (Allinger, N. L. *J. Am. Chem. Soc.* **1977**, *99*, 8127) mainly in the use of partial charges on atoms, instead of bond dipoles, and in the absence of unshared pairs of electrons on certain nitrogen and oxygen atoms.